

Project description

Contents

1	Science	2
2	Research hypothesis	3
3	Objectives	5
4	Scientific originality	7
5	Relevance to the research field	8
6	Method	9
6.1	Final states and observables	9
6.2	Event selection and categorization	10
6.3	Neutrino reconstruction	12
6.4	Multivariate analysis	14
6.5	Sensitivity results	15
6.6	Possible extensions of ideas	16
7	Planned cooperation arrangement	17
8	Work and plan	17
9	Ethical, safety-related or regulatory aspects	20
10	Sex-specific and gender related issues	21
11	Human resources	21
Annex 1	References	23
Annex 2	Research institution and required funding	27
Annex 3	CV of the principal investigator	29

1 Science

Since the start of operations in 2008, the Large Hadron Collider (LHC) at CERN has provided a data set amounting to $\approx 10^{16}$ collisions that is expected to double, once more, until 2024. During the LHC Run 2 (2015–2018), the CMS experiment [1] collected 137 fb^{-1} of proton-proton collision data and is now performing extensive analyses to extract the maximum knowledge on fundamental particle physics processes at the TeV scale. The most prominent key milestone in the LHC experiments’ history is the discovery of the Higgs boson (H), jointly announced by the ATLAS and CMS collaborations in 2012 [2, 3]. It completed the particle content of the standard model (SM) of particle physics. Since then, precision measurements of the Higgs boson’s mass [4, 5], its charge-parity (CP) nature [6, 7], its couplings to gauge bosons (W, Z, γ), and other couplings have been at the center of the LHC research program with many already entering the precision regime. At the same time, the lack of smoking-gun evidence for resonant phenomena beyond the SM (BSM) has discouraged many sophisticated models that were conceived to cure, at various degrees, the SM’s shortcomings. Supersymmetry, a viable model of dark matter candidate or models with extra dimensions have not been discovered.

Is the case, therefore, closed? In this proposal, we argue on the contrary. In fact, the recent advent of effective field theories (EFT) [8–10] demonstrates impressively that subtle deviations, hiding in the observables’ distributions, can probe BSM phenomena at energy scales often exceeding the LHC’s reach in the direct searches. The underlying theoretical framework is the SM effective field theory (SM-EFT) [11–15] that systematically extends the SM with operators of higher mass dimension that smoothly change the kinematic spectra. Specifically, SM-EFT modifications to the SM Higgs sector result in deviations that grow with the momenta of the final state particles. The joint production of a H boson and a vector boson (VH with $V = W^\pm, Z$) are particularly strongly affected, turning the highly energetic VH final states into extremely important discovery tools for BSM phenomena. In addition, BSM sources of CP violation change subtle triple-correlations of angular observables that are easily lost if not targeted explicitly by means of “interference resurrection” [16]. The latter techniques have been demonstrated in the simpler $W\gamma$ final states [17], but the order-of-magnitude sensitivity gain for precision measurements, although proposed recently [18], has not been exploited experimentally in the Higgs sector.

To close these gaps, I propose an extensive measurement of the H–V couplings in VH final states. Resurrecting the process’ interference pattern and simultaneously leveraging the energy growth in the kinematic tails of the H, W^\pm , and Z bosons promise unique sensitivity and a wide reach to SM-EFT effects, including the CP coupling structure. The proposed analysis includes differential cross section measurements of a number of observables never considered before. Combining H boson decays to a pair of b quarks with the requirement of leptonic V decays (electrons or muons) leads to a high signal acceptance while suppressing the difficult hadronic backgrounds.

The work can start with the data set already collected during the LHC’s Run 2. With the additional 160 fb^{-1} data to be delivered by LHC in Run 3 (2022–2024), these

measurements are expected to have a significant leap in precision. In the remainder of the proposal, I attempt to demonstrate these claims.

2 Research hypothesis

I assume that TeV scale phenomena are described by the standard model effective theory (SM-EFT). The SM-EFT progressively includes operators of mass dimension greater than four that respect the SM symmetries [11–15] and is defined by the Lagrangian

$$\mathcal{L}_{\text{SM-EFT}} = \mathcal{L}_{\text{SM}} + \sum_i \frac{c_i^{(5)}}{\Lambda} \mathcal{O}_{5,i} + \sum_i \frac{c_i^{(6)}}{\Lambda^2} \mathcal{O}_{6,i} + \dots \quad (2.1)$$

It captures all non-resonant BSM phenomena below an arbitrarily chosen energy scale Λ . The dimensionless Wilson coefficients c are used to parameterize the effects on observables, while the terms $\mathcal{O}_{5,6}$ are the operators at mass dimension 5 and 6, respectively. The only possible dimension-5 candidate is the Weinberg operator [19], not relevant for the phenomenology of this proposal [20]. The number of baryon- and lepton number conserving dimension-6 operators is 2499 when all flavor degrees of freedom are counted. There are 76 operators respecting a $U(3)^5$ flavor symmetry [12] among which the 12 in Table 1 affect the VH process. The operators are written in the so-called Warsaw-basis basis [21], and it is the central aim of this proposal to constrain their Wilson coefficients via their numerous effects on the Higgs boson production properties and decay kinematics [22–25].

Table 1: The dimension-6 operators in the Warsaw basis [21] affecting VH processes.

$\mathcal{O}_{Hq}^{(1)}$	$iH^\dagger \overleftrightarrow{D}_\mu H \bar{q} \gamma^\mu q$	\mathcal{O}_{HWB}	$H^\dagger \sigma^a H W_{\mu\nu}^a B^{\mu\nu}$
$\mathcal{O}_{Hq}^{(3)}$	$iH^\dagger \sigma^a \overleftrightarrow{D}_\mu H \bar{q} \sigma^a \gamma^\mu q$	$\mathcal{O}_{H\tilde{W}B}$	$H^\dagger \sigma^a H W_{\mu\nu}^a \tilde{B}^{\mu\nu}$
\mathcal{O}_{Hu}	$iH^\dagger \overleftrightarrow{D}_\mu H \bar{u}_R \gamma^\mu u_R$	\mathcal{O}_{HW}	$ H ^2 W_{\mu\nu} W^{\mu\nu}$
\mathcal{O}_{Hd}	$iH^\dagger \overleftrightarrow{D}_\mu H \bar{d}_R \gamma^\mu d_R$	$\mathcal{O}_{H\tilde{W}}$	$ H ^2 W_{\mu\nu}^a \tilde{W}^{a\mu\nu}$
\mathcal{O}_{HD}	$(H^\dagger D_\mu H)^* (H^\dagger D_\mu H)$	\mathcal{O}_{HB}	$ H ^2 B_{\mu\nu} B^{\mu\nu}$
$\mathcal{O}_{H\Box}$	$(H^\dagger H) \Box (H^\dagger H)$	$\mathcal{O}_{H\tilde{B}}$	$ H ^2 B_{\mu\nu} \tilde{B}^{\mu\nu}$

The operators $\mathcal{O}_{Hq}^{(1)}$, $\mathcal{O}_{Hq}^{(3)}$, \mathcal{O}_{Hu} , and \mathcal{O}_{Hd} introduce the 4-point interactions depicted in Fig. 1 (left). Together with \mathcal{O}_{HD} and \mathcal{O}_{HWB} , these six operators describe all relevant V-fermion coupling modifications (Fig. 1, middle). The remaining operators modify the H–V coupling, shown in Fig. 1 (right). There is also the Yukawa-type operator $H^\dagger H \bar{Q} H b$, which only changes the $H \rightarrow b\bar{b}$ branching ratio and, thus, can be probed in an inclusive cross section measurement.

The $SU(2)$ doublet H is expanded as $\begin{pmatrix} 0 \\ v + h \end{pmatrix}$, where v is the vacuum expectation value and h corresponds to the physical Higgs boson. At weak scale, H is replaced by v

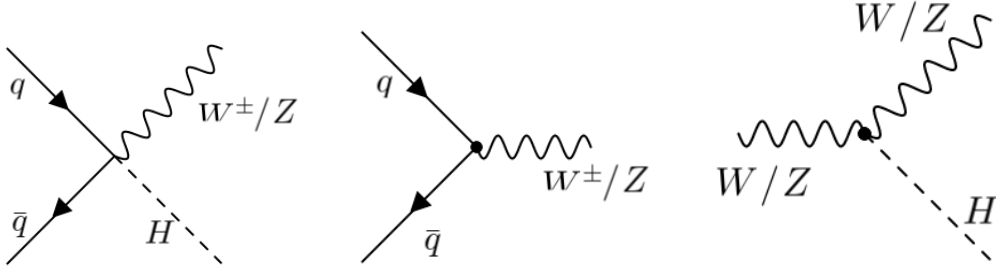


Figure 1: Feynman diagrams for VH production sensitive to different dimension-6 operators. The energy growth induced by the diagrams in VH production cross section are the following: E^2 (left), E^0 (middle), E (right).

in operators in Table 1, and some of them can be constrained using the existing collider results from the LEP and the Tevatron experiments. Nevertheless, the expected bounds from the LHC are expected to be more stringent [26, 27]. Moreover, the operators of the form $H^2 \mathcal{L}_{\text{SM}}$, can be directly probed for the first time at LHC [28].

The Feynman diagram with four-point interaction (Fig. 1, left) involves one scalar and one vector field, each with mass dimension one and two fermion fields, each with mass dimension three halves. Power counting with naive dimensional analysis [29] implies that this causes an energy growth of E^2 in cross section. Similarly, after replacing H by the diagram with the modification with fermion–V coupling (Fig. 1, middle) corresponds to Lagrangian expansion of the form $\frac{v^2}{\Lambda^2} V_\mu \bar{\psi} \gamma^\mu \psi$ and does not that induce an energy growth in cross section. The operators modifying H–V coupling (Fig. 1, right) give rise to terms $vh\partial^\mu \partial^\nu V_\mu V_\nu$. When interfering with the SM term $((H^\dagger H)V^\mu V_\mu)$ gives rise to a linear energy growth in cross section. The proposed measurement will probe the operators in Table 1 using kinematic variables exhibiting energy growth and, for the first time, the angular structure that is sensitive to subtle interference effects. At high energy, since H has large p_T , its decay products are collimated and can be reconstructed using large-sized jets, thus providing a testbed for the application of the cutting-edge jet substructure techniques [30, 31]. For the angular information, we exploit the techniques of Ref. [18] and define the angles and decay planes of the VH process as shown in Fig. 2.

The squared amplitude of $V (\rightarrow \ell\ell)H (\rightarrow b\bar{b})$ production, when summing over the lepton helicities, has the following form

$$|\mathcal{M}(\hat{s}, \Theta, \theta, \varphi)|^2 = \sum_i a_i(\hat{s}) f_i(\Theta, \theta, \varphi) , \quad (2.2)$$

where $a(\hat{s})$'s are functions of Wilson coefficients and the energy transfer involved in the process (\hat{s}) and f 's, functions of three angles, have the following forms with indices referring to the polarizations of the intermediate vector boson:

$$\begin{aligned} f_1 &= f_{LL} = \sin^2 \Theta \sin^2 \theta, \\ f_2 &= f_{TT}^1 = \cos \Theta \cos \theta, \end{aligned}$$

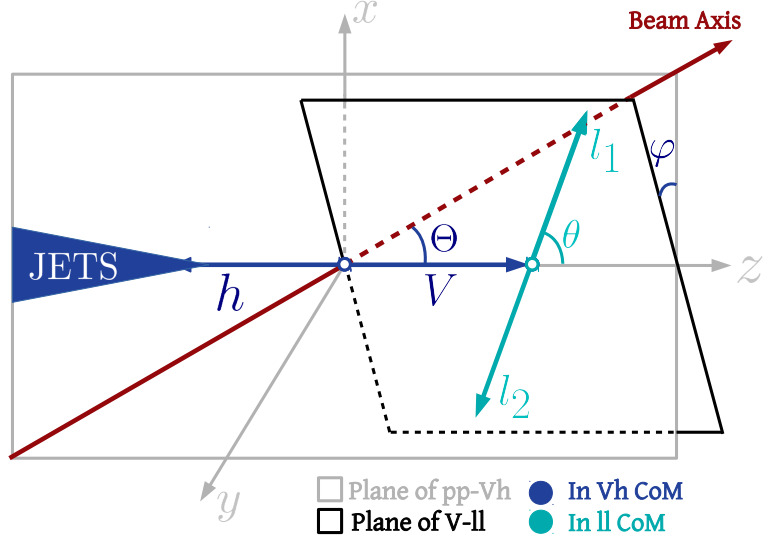


Figure 2: Decay planes and angles in the $V (\rightarrow \ell\ell)H (\rightarrow b\bar{b})$ production. Note that Θ is defined in the VH rest frame, while θ is defined in the V rest frame.

$$\begin{aligned}
f_3 &= f_{TT}^2 = (1 + \cos^2 \Theta)(1 + \cos^2 \theta), \\
f_4 &= f_{LT}^1 = \cos \varphi \sin \Theta \sin \theta, \\
f_5 &= f_{LT}^2 = \cos \varphi \sin \Theta \sin \theta \cos \Theta \cos \theta, \\
f_6 &= \tilde{f}_{LT}^1 = \sin \varphi \sin \Theta \sin \theta, \\
f_7 &= \tilde{f}_{LT}^2 = \sin \varphi \sin \Theta \sin \theta \cos \Theta \cos \theta, \\
f_8 &= f_{TT'} = \cos^2 \varphi \sin^2 \Theta \sin^2 \theta, \\
f_9 &= \tilde{f}_{TT'} = \sin^2 \varphi \sin^2 \Theta \sin^2 \theta.
\end{aligned} \tag{2.3}$$

A traditional inclusive measurement integrating over Θ, θ, φ makes all the terms in Eq. (2.3), except f_{LL} and f_{TT}^2 , vanish, causing a loss of important information, which can only be recovered using a triple differential analysis with respect to all three angles. One point to note here is that the absence of knowledge about the direction of incoming quark and anti-quark makes the terms in Eq. (2.2) corresponding to f_{TT}^1, f_{LT}^1 , and \tilde{f}_{LT}^1 vanish.

3 Objectives

The goal of this proposal is to probe the SM-EFT operators in Table 1 as precisely as possible using events from the VH processes in the data from the CMS experiment. The experimental work to excavate two distinct features, combined to achieve optimal sensitivity, are tackled separately.

In the first objective, I will exploit energy growth induced by 4-point SM-EFT interactions to boost the sensitivity of the differential cross section measurements in the leptonic

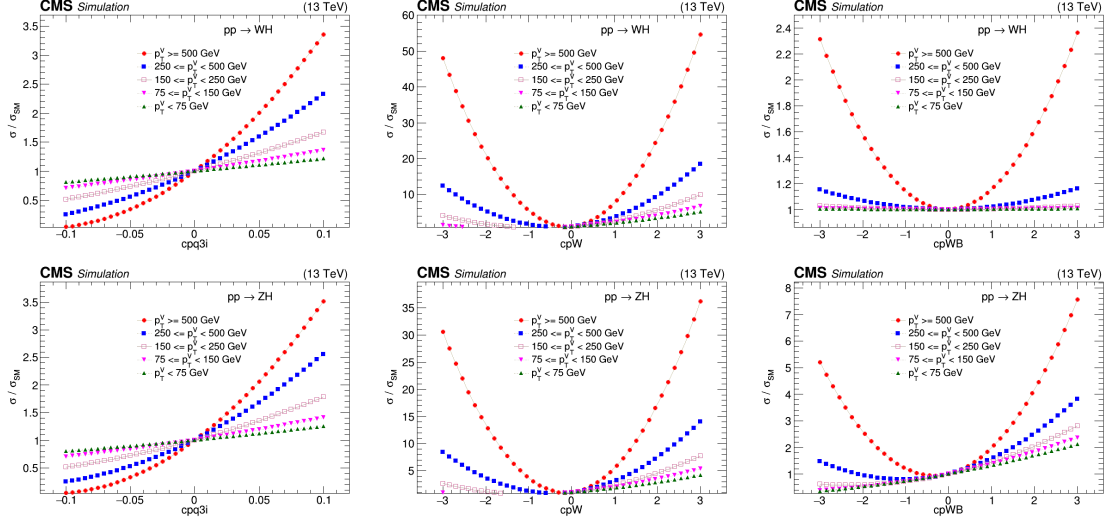


Figure 3: The ratio $\sigma/\sigma_{\text{SM}}$ of the cross section of the WH (top) and ZH (bottom) processes relative to the SM prediction as a function of Wilson coefficients $\mathcal{O}_{Hq}^{(3)}$ (left), \mathcal{O}_{HW} (middle), and \mathcal{O}_{HWB} (right) in five regions of W and Z boson p_T , respectively.

VH final states. Latest jet substructure techniques for boosted objects will be applied to exploit the energy growth. The three operators $\mathcal{O}_{Hq}^{(3)}$, \mathcal{O}_{HW} , \mathcal{O}_{HWB} , their CP-odd counterparts, and the operators \mathcal{O}_{HD} , $\mathcal{O}_{H\Box}$ affect both WH and ZH productions. I show the dependence of the production cross section on the first three Wilson coefficients for different selections in vector boson transverse momentum, $p_T(V)$, in Fig. 3. The energy growth is visible as an increased dependence on the Wilson coefficient for selections with higher $p_T(V)$. The operators $\mathcal{O}_{Hq}^{(1)}$, \mathcal{O}_{Hu} , \mathcal{O}_{Hd} , \mathcal{O}_{HB} , and $\mathcal{O}_{H\bar{B}}$ affect only the ZH production, because both left- and right-handed initial-state quarks of same flavor take part in ZH production, while only the left-handed quarks of different flavors are involved in WH production [32, 33]. In the second objective, I use the angular observables to further boost the sensitivity and tackle the CP-structure of the V–H interaction. As an example, I show one of the angular variables, ϕ , in Fig. 4. Here, the leading contribution for the CP-even and -odd operators come from the terms corresponding to f_{LT}^2 and \tilde{f}_{LT}^2 in Eq. (2.3), respectively, which have $\cos(\varphi)$ and $\sin(\varphi)$ dependence. In the simpler $W\gamma$ final state, the technique increased the sensitivity by about a factor of 10 [17].

The SM cross section for WH production with $H \rightarrow b\bar{b}$ and $W \rightarrow \ell\nu$ is 0.28 pb, whereas it is only 0.05 pb for ZH production, where $Z \rightarrow \ell\ell$. Thus, W process thus provides better statistical precision in the measurements. The Z final state is less populated, but backgrounds are relatively smaller, particularly at high energy, providing independent and corroborating evidence of the BSM signal. Also, as mentioned previously, ZH production is affected by a number of operators which do not participate in WH production because of the helicity structure of incoming quarks. Therefore, simultaneous measurements of the

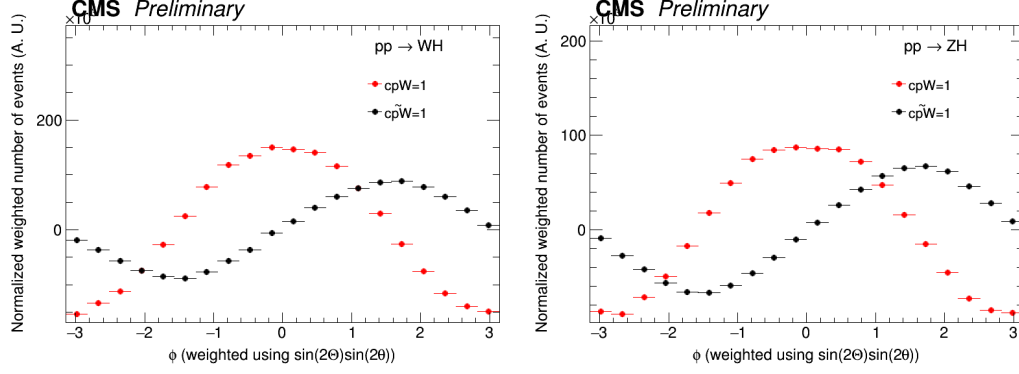


Figure 4: Distribution of angle ϕ for CP-even operator \mathcal{O}_{HW} (red points) and CP-odd operator $\mathcal{O}_{H\tilde{W}}$ (black points) at the particle level in case of WH (left) and ZH (right) productions.

couplings in both WH and ZH processes are necessary to confidently probe the complete set of operators relevant [18]. A preliminary sensitivity study is presented in Sec. 6.

4 Scientific originality

The combined data sets from the LHC Run 2 and the future LHC Run 3 provide an opportunity to measure SM-EFT operators involving the Higgs field [28, 34] with unprecedented precision. In the $V \rightarrow \ell\ell$ and $H \rightarrow b\bar{b}$ final state, I extend traditional search strategies, based on the basic STXS binning scheme [35], by angular observables sensitive to subtle SM-EFT effects and the CP-structure of the V–H interaction. For the first time,

- the complete multi-dimensional event information is used in VH production to directly probe dimension-6 SM-EFT operators inducing energy growth. Besides kinematic event properties, novel angular variables (Fig. 6) crucially refine the analysis strategy. They disentangle the various SM-EFT effects and can largely boost the sensitivity [17]. Furthermore,
- the angular information, not explored previously in VH production, is used to probe the CP structure of SM-EFT modifications of the V–H coupling. We can, therefore, measure new sources of CP violation beyond the SM.

Smaller novel items pertain to the multivariate (MVA) analysis strategy employed to achieve these goals. For example, the proposer’s group has recently developed a new technique to train tree-based classifiers to optimally separate effects of SM-EFT operators from the SM background [36].

5 Relevance to the research field

On a broad scale, the measurements provide a new piece of the TeV-scale SM-EFT puzzle. The findings will be interpreted in the context of SM-EFT, which guarantees maximal independence from model assumptions and a smooth interface with theory interpretations.

The absence of hints for resonant BSM phenomena has shifted the focus from ultraviolet-complete theories to EFTs, with first attempts at complete TeV-scale characterizations emerging relatively recently [37–39]. At the experimental collaborations, the measurements of SM-EFT operator coefficients has just arrived at the center stage of the LHC physics program [40–42]. The interest from the theoretical and experimental communities is still growing, reflected in various new working groups (e.g. the LHC EFT working group [43]) and lecture series (e.g., “All things EFT” [44]).

In particular, the proposed research contributes a unique probe of SM-EFT operator coefficients in the Higgs sector. Besides the sensitivity boost from novel experimental techniques, it also complements the existing results by extending to CP-sensitive angular observables, tightly constraining the V–H couplings. A deviation from the SM hinting at new sources of CP-violation will have wide-ranging significance in the explanation of the origin of the matter-antimatter asymmetry of the universe [45–47].

The relevance of the proposed research extends to adjacent fields when the interplay of LHC measurements in global SM-EFT measurements is considered [37, 39]. For example, specific assumptions of the BSM flavor structure provides a tight connection of the proposed measurement with the sector of top-quark physics. Moreover, the SM electroweak symmetry breaking relates the 4-point interactions in Table 1 to complementary measurements of the fermion-gauge boson couplings. An example of this link can be obtained from Fig. 1 (left) when replacing the H boson line with v .

The results obtained from the proposed measurements can also be reinterpreted as constraints on ultraviolet-complete new physics models describing the underlying dynamics at high energy. Particular models the proposed analysis will be capable of probing are the following:

- Singlet scalar models, where a scalar field, singlet under the SM gauge group, is introduced [48, 49]. This class of models gives rise to operators of the form of $\mathcal{O}_{H\Box}$, \mathcal{O}_{HD} , \mathcal{O}_{HW} , \mathcal{O}_{HB} , \mathcal{O}_{HWB} , \mathcal{O}_{Hu} , and \mathcal{O}_{Hd} .
- Models predicting the existence of a new vector boson [50], for example, Z' and W' . The models with extra spatial dimensions [51], and little Higgs models [52] fall in this category. If the new bosons coupling to both fermions and gauge bosons has large mass ($> \text{few TeV}$), they give rise to the contact interaction shown in Fig. 1 (left) and thus contributes to the operators $\mathcal{O}_{Hq}^{(1)}$, $\mathcal{O}_{Hq}^{(3)}$, \mathcal{O}_{Hu} , and \mathcal{O}_{Hd} .
- Colored extensions of the SM with vector-like quarks (VLQs), triplet under $SU(3)$ and singlet under $SU(2)_L$ [53, 54]. When VLQs are allowed to couple to light quarks, they can give rise to $\mathcal{O}_{Hq}^{(1)}$ and $\mathcal{O}_{Hq}^{(3)}$ operators. Particularly, new physics models with Z' or VLQs are in highlights in recent times to explain the anomalies in the flavor sector.

The phenomenological implications of the V–H coupling measurement thus radiate into neighboring research areas, while the proposed experimental program is self-contained. In the following section, I aim to prove that.

6 Method

We target to utilize the combined data set from the LHC Run 2, corresponding to an integrated luminosity of 139 fb^{-1} at $\sqrt{s} = 13 \text{ TeV}$, and the LHC Run 3, currently estimated at $\approx 160 \text{ fb}^{-1}$. With 45% of the data available, we can develop and publish novel analysis techniques during the third running period. When the full data set is available at the end of Run 3, we can obtain ultimate precision on a comparably short time scale and publish a benchmark result whose precision can not be surpassed until well into the HL-LHC research program.

In the following, we report the results of a feasibility study of the proposed measurements. While the clean ZH process serves as an independent search channel with orthogonal SM-EFT sensitivity, we focus on the more challenging WH final states. The results are equally valid for the ZH case.

6.1 Final states and observables

In the SM, the $H \rightarrow b\bar{b}$ decay channel has the largest branching ratio, motivating to choose it as a focus for improving the statistical precision of the measurement. Leptonic decay modes of the vector bosons help in reducing difficult backgrounds from the multijet production in quantum chromodynamics (QCD). In summary, we consider the WH and ZH production processes in the $W \rightarrow \ell\nu$, $Z \rightarrow \ell^+\ell^-$, and $H \rightarrow b\bar{b}$ decay channels, where $\ell = (e, \mu)$.

As shown in Sec. 3 and Fig. 3, the 4-point interactions provided by the operators in Table. 1 induce energy growth, modifying the highly energetic tail of distributions of kinematic observables such as the transverse boson momenta, $p_T(W)$, $p_T(Z)$, or $p_T(H)$. These kinematic observables alone are not sufficient to disentangle the various effects from a large number of possible SM-EFT operators. A systematic analysis of helicity amplitudes in VH production decay is provided in Ref. [18]. Amplitudes involving the longitudinal and transverse vector boson polarizations contribute differently to VH production in both the SM and in SM-EFT. The interference among helicity amplitudes, including CP effects, is preserved at the event level in subtle angular triple-correlations. For example, the cosinusoidal and sinusoidal modulations in ϕ distributions shown in Fig. 4 are obtained after using the sign of $\sin(2\Theta)\sin(2\theta)$ as seen from \tilde{f}_{LT}^2 and f_{LT}^2 terms, respectively in Eq. 2.3. This allows to extract rich information about the event structure from a joint analysis of kinematic and angular variables.

Specifically, Ref. [18] proposes to reconstruct the novel angular variables shown in Fig. 2. It is important to note that traditional strategies can not leverage the subtle angular triple-correlation: integrating over any of the angles in the final observables removes the interference effects [16].

6.2 Event selection and categorization

The CMS trigger system selects the VH events based on the presence of leptons (electrons or muons) originating from the W or Z bosons. At moderate momenta, single- and double-lepton triggers are used. At high $p_T(V)$, backup trigger paths requiring considerable hadronic activity are used to recover efficiency losses for events with highly asymmetrical V decay or with a highly energetic electron.

The measurement of the trigger selection efficiency ratio between data and simulation is a standard (but important) step towards reducing the total systematic uncertainty. For this purpose, we use tag-and-probe methods with $Z \rightarrow \ell^+ \ell^-$ events to obtain event-level correction factors that scale the simulation to the data. For the remainder of the feasibility study, we assume that simulation correctly predicts the trigger selection efficiency. All results are obtained from events generated with `Madgraph5_aMC@NL0` [55] and simulated up to the CMS detector level. The SM-EFT effects are incorporated with `MadWeight` [56] and using the `SMEFTsim` model [57].

After the trigger decision, we select WH candidate events by requiring an electron or a muon with $p_T > 32$ and > 25 GeV, respectively. The CMS identification lepton criteria in the Run 2 data set correspond to 90 and 95% efficiency for genuine electrons and muons, respectively. As will be discussed in Sec. 6.3, the four-momentum of the neutrino from the W decay is reconstructed using the missing transverse momentum vector (\vec{p}_T^{miss}), assuming that the invariant mass of neutrino-lepton system equals m_W .

A sample enriched in boosted W bosons is selected by the requirement $p_T(W) > 150$ GeV. After this selection, the level of QCD multijet production is negligible. Requiring a minimum difference of the azimuthal lepton- and p_T^{miss} angles, $\Delta\phi(\ell, \vec{p}_T^{\text{miss}}) > 2$, removes events with spurious signals while retaining good signal efficiency. Finally, W candidate events must not contain additional electrons or muons with $p_T > 25$ GeV.

The selected events are further categorized into measurement regions depending on quantities from the jet system. If the H boson has large p_T , its decay products are merged into a jet with a large cone size. In this “boosted topology”, the H boson is reconstructed and identified in a the set of jets provided by the anti- k_T algorithm with the distance parameter of $R = 0.8$ (AK8 jets). Otherwise, the H boson is in the “resolved topology” where it can be reconstructed using standard AK4 jets originating from the b quark pair. In the boosted topology, the deep neural network (DNN) based algorithms DeepJet [58] and DeepAK8 [31] are used to identify AK4 jets in the AK8 jet that correspond to the b quark pair. The DeepAK8 tagger provides probability-normalized classifier values for the top quark, W boson, light quark or gluon hypothesis for each AK8 jet. We use this information later on for signal-to-background discrimination in the boosted topology.

In the resolved topology, the two AK4 jets with highest b tagging scores, referred to as $b_{1(2)}$, form the H candidate, while the AK8 jet (J) with the highest H tagging score provides the H candidate in the boosted topology. For AK8 jets, soft drop grooming [59] is used to calculate the mass by removing the uncorrelated radiation clustered into the jet. The signal region (SR), enriched by $W (\rightarrow \ell\nu) H (\rightarrow b\bar{b})$ events, is constructed using the conditions listed in Table 2.

Table 2: Selection conditions targeted for WH events.

Resolved category	Boosted category
At least 2 b-tagged AK4 jets (satisfying $p_T > 30 \text{ GeV}$, $ \eta < 2.5$)	At least 1 AK8 jets (satisfying $p_T > 250 \text{ GeV}$, $ \eta < 2.5$)
The b tagging score of $b_1 > \text{btag}_{\text{max}}^{\text{cut}}$	The H tagging score of $H > \text{Htag}^{\text{cut}}$
The b tagging score of $b_2 > \text{btag}_{\text{min}}^{\text{cut}}$	
Up to 1 additional AK4 jets	Veto on extra b-tagged AK4 jets
$M(b_1 + b_2) \in [90, 150] \text{ GeV}$	Soft-drop mass of $J \in [90, 150] \text{ GeV}$

In Table 2, the threshold values $\text{btag}_{\text{max}}^{\text{cut}}$ and $\text{btag}_{\text{min}}^{\text{cut}}$ are chosen to ensure a DeepJet b-tagging mistag rate of 1% and 10% for light quark or gluon jets, respectively. The threshold value Htag^{cut} corresponds to a H mistag rate of 1%.

Inverting specific requirements in Table 2, defines control regions (CRs), enriched by the various background processes. For example, requiring two or more AK4 jets in the resolved category or the presence of b-tagged AK4 jets in the boosted category selects an event sample enriched with top quark pair production ($t\bar{t}$). Inverting the mass window on the H candidate results in a CR dominated by vector boson production in association with b- and c-quark jets ($W + b/c$). Finally, resolved (boosted) events failing the requirement of the presence of two b-tagged AK4 jets (one Higgs-tagged AK8 jet) are dominated by vector boson production in association with light quark or gluon jets ($W + \text{udsg}$). These CRs are used to measure and validate the corresponding backgrounds in data.

The distribution of $p_T(W)$ in the resolved and boosted SR are shown in Fig. 5, where alternate WH signal hypothesis for the operators $\mathcal{O}_{Hq}^{(3)}$ and \mathcal{O}_{HW} are overlaid. The figure shows the importance of the $t\bar{t}$, $W + b/c$, and $W + \text{udsg}$ backgrounds in the WH SRs.

Next, we turn to the sensitivity of the angular observables. As shown in Fig. 6, the SM production, dominated by longitudinal polarization of W boson, exhibits differences in Θ for nonzero \mathcal{O}_{HW} coefficients because this operator enhances the helicity amplitude of VH production with transverse polarizations. The observable ϕ , on the other hand, is very sensitive to the CP-nature of the V-H coupling and the difference in the modulation of CP-even and CP-odd operator coefficients is clearly visible. The CP-sensitivity in the ϕ observable is slightly affected by the ambiguities introduced by the unknown z momentum of the neutrino entering the W momentum reconstruction. This necessitates the development of a sophisticated algorithm for neutrino reconstruction, possibly similar to the MVA-based technique designed in top quark analyses for assigning reconstructed objects to particles produced in the hard interaction [60]. The ϕ observable is weighted by $\sin 2\Theta \sin 2\theta$ to lift the cancellation otherwise enforced by the triple angular correlation. For the first time, we thus resurrect the interference of the helicity amplitude in H final states at the detector level. Comparing these predictions to the Run 2 and 3 data from the CMS experiment is a central goal of the proposal.

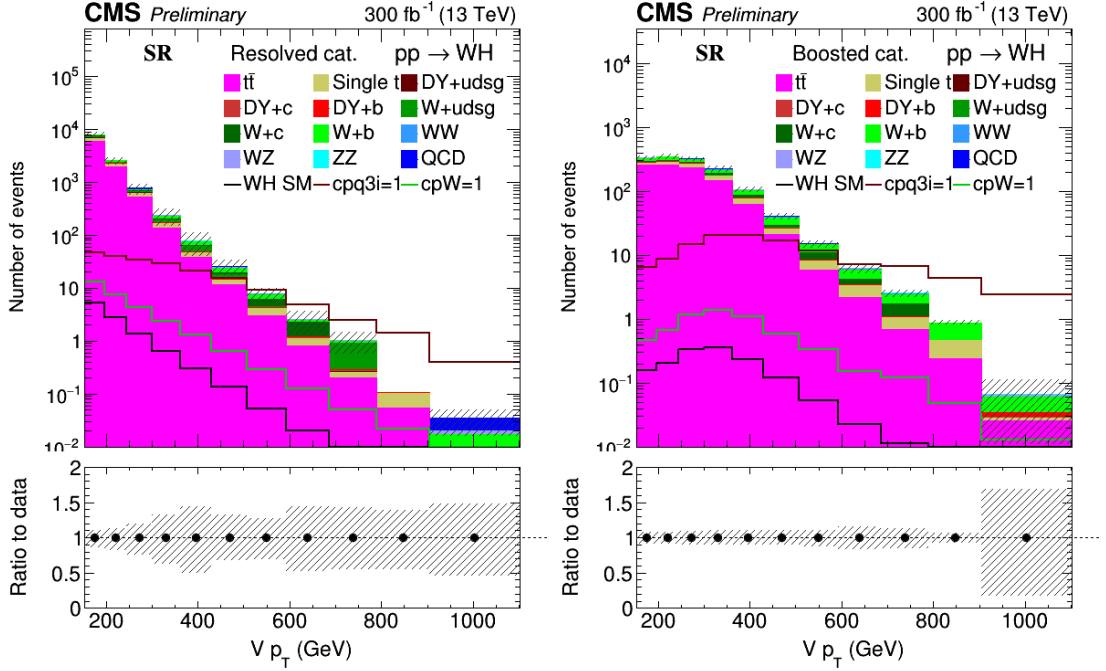


Figure 5: Distribution of W boson p_T in the resolved (left) and boosted (left) categories of the SR. Impact of systematic uncertainties on jet energy scale and resolution, correction factor used to match the b-tagging and Higgs-tagging efficiencies in data and simulation are shown in the bottom panel.

6.3 Neutrino reconstruction

In order to reconstruct the momentum of invisible neutrino in $W \rightarrow \ell \nu$, we assume that the ν is the only source of \vec{p}_T^{miss} in the event and regard p_T and ϕ of \vec{p}_T^{miss} to be the same of ν . In a simple approach, we use the quadratic equation from the W-mass constraint to calculate $\eta(\nu)$. The two possible solutions are

$$\eta(\nu) = \eta(\ell) \pm \cosh^{-1}(1 + \Delta^2), \text{ where} \quad (6.1)$$

$$\Delta^2 = \frac{m_W^2 - m_T^2(\ell, p_T^{\text{miss}})}{2p_T^{\ell} p_T^{\text{miss}}}. \quad (6.2)$$

Large $p_T(W)$ leads to $\Delta \ll 1$, and the two solutions become

$$\eta(\nu) \simeq \eta(\ell) \pm \sqrt{2}\Delta + \mathcal{O}(\Delta^3). \quad (6.3)$$

In this limit, the angular variable θ and Θ converge to the same values, whereas a two-fold ambiguity $\phi_+ \simeq \pi - \phi_-$ remains for ϕ . This ambiguity is visible in Fig. 7 and currently reduces the CP-sensitivity in WH production. No attempt was made to reduce the impact of the ambiguity for the purpose of this proposal. As part of the analysis development, we will develop a multi-variate discriminator to select the correct solution based on the kinematic event properties.

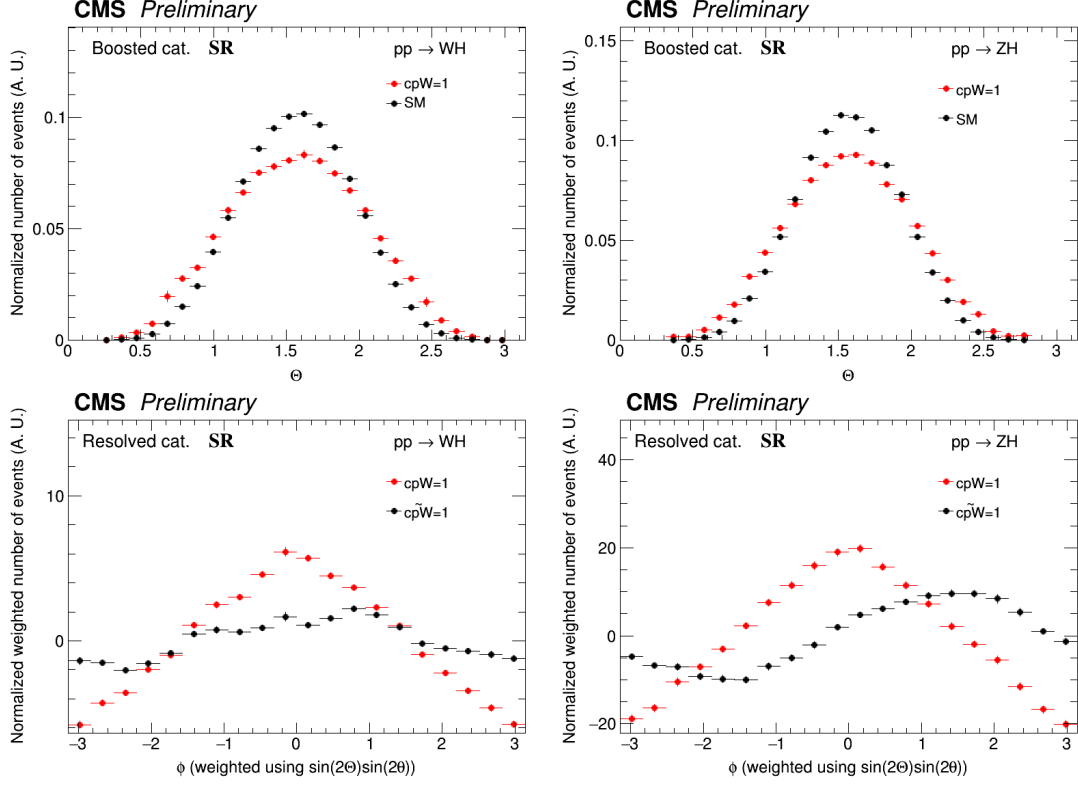


Figure 6: Normalized distribution of polar angle Θ in WH (top left) and ZH (top right) productions for $cpW = 1$ and SM scenarios in the boosted category. Normalized distribution of azimuthal angle ϕ in WH (bottom left) and ZH (bottom right) productions for $cpW = 1$ and $cp\tilde{W} = 1$, respectively; SM component is subtracted from in these distributions.

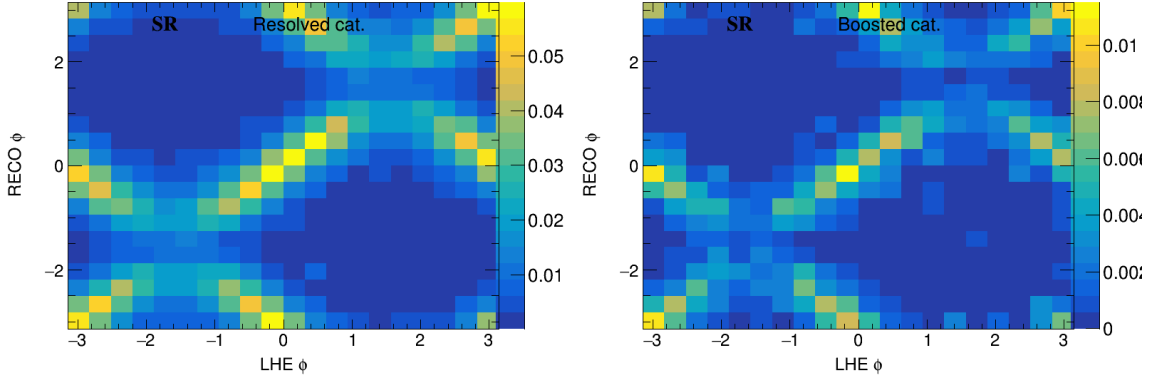


Figure 7: Correlation between ϕ calculated at parton level and detector level in the resolved (left) and boosted (right) categories in WH production.

Table 3: Input variables to the MVA discriminator designed to separate events from VH and $t\bar{t}$ productions.

Lepton-specific variables for WH (left) and ZH (right) signals.	
p_T component of \vec{p}_T^{miss}	p_T and η of the leading lepton
p_T and η of the lepton	p_T and η of the subleading lepton
$\Delta\phi(\ell, \vec{p}_T^{\text{miss}})$	$\Delta\phi(\ell_1, \ell_2)$
$\Delta\phi(W, H)$	$\Delta\phi(Z, H)$
Event thrust (see definition in [61])	Event thrust

Variables characterizing the jet system in resolved (left) and boosted (right) categories.

B-tagging scores of b_1 and b_2	DeepAK8 top tagging score
$\text{Min}(p_T(b_1), p_T(b_2))$ and b_2	DeepAK8 W tagging score
$\text{Max}(p_T(b_1), p_T(b_2))$	DeepAK8 $b\bar{b}$ tagging score
$\text{Max}(p_T(b_1)/p_T(\ell), p_T(b_2)/p_T(\ell))$	Rapidity and mass of H candidate
$\Delta\phi(b_1, b_2)$	
Rapidity and mass of H candidate	
AK4 jet multiplicity	
(satisfying $p_T > 30 \text{ GeV}$, $ \eta < 2.5$)	

6.4 Multivariate analysis

As shown in Fig. 5, the SRs are subject to significant backgrounds from top quark pair and vector boson production in association with jets. To separate the WH and ZH signals optimally from the backgrounds, MVA discriminators are constructed. In this study, it comprises two fully connected dense layers, while the discriminator will be promoted to a DNN in the analysis with real data. A very preliminary set of input variables is listed in Table 3. Variables in two columns in the upper group are used for the extraction of WH and ZH signals, respectively, while left and right columns in the lower group list variables characterizing the jet system in the resolved and boosted categories, respectively, for the separation of both WH and ZH signals from $t\bar{t}$ background.

Normalized distributions of MVA discriminators in SM WH and $t\bar{t}$ events are shown in Fig. 8. The output discriminator shapes and the performance of the discriminator, quantified with ROC curves [62], are shown in Fig. 8. Benefiting from the DeepAK8 tagger outputs, the discriminator constructed in the boosted category performs slightly better. In both cases, the signal distribution is sharply peaked at high discriminator values, indicating a successfully trained classifier. In the next section, we quantify the sensitivity gain from this strategy.

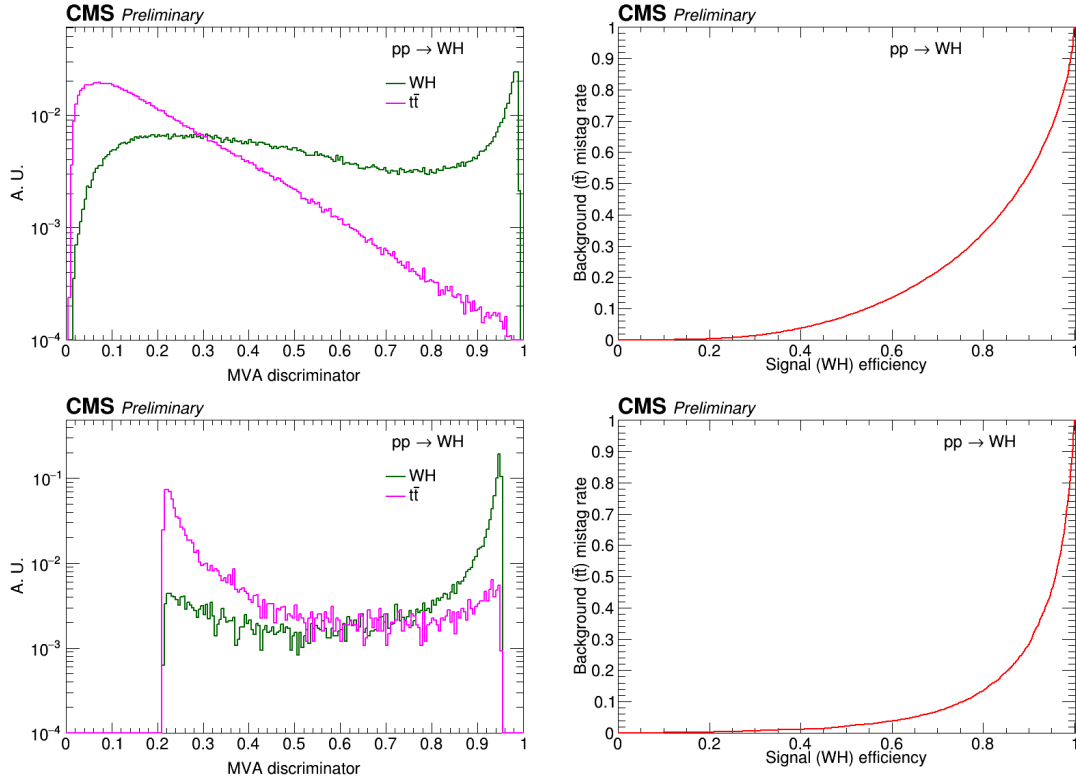


Figure 8: Normalized distributions of the MVA discriminator in signal (WH) and background ($t\bar{t}$) events (left) and ROC curve characterizing the performance of MVA discriminator (right) in the resolved (top) and boosted (bottom) categories.

6.5 Sensitivity results

Although the final condition on the MVA discriminator is subject to development during the project, we can obtain a simple assessment of the sensitivity with a threshold on the MVA discriminator corresponding to a signal efficiency of 80%. This choice corresponds to a background efficiency of $\sim 30\%$ ($\sim 15\%$) in the resolved (boosted) category. Next, we perform one-dimensional likelihood scans for the three Wilson coefficients corresponding to the operators $\mathcal{O}_{Hq}^{(3)}$, \mathcal{O}_{HW} , and $\mathcal{O}_{H\tilde{W}}$, respectively, while setting all other Wilson coefficients to 0. Normalizing the predicted yields to an integrated luminosity of 300 fb^{-1} , we show the negative log-likelihood results in in Fig. 9. Fig. 9 shows that a large gain in sensitivity is obtained by adding the boosted category due to the energy growth induced by the operators: The Wilson coefficient corresponding to $\mathcal{O}_{Hq}^{(3)}$ can be constrained to percent level and the ones corresponding to \mathcal{O}_{HW} and $\mathcal{O}_{H\tilde{W}}$ within tens of percent at 95% confidence level with luminosity amounting to 300 fb^{-1} . Quantitative bounds are presented in Table 4 at 68% confidence level. An improvement due to a binning in ϕ is obtained in the resolved category. Simultaneous use of information about all three angles Θ , θ , ϕ is expected to result in a large increase in sensitivity.

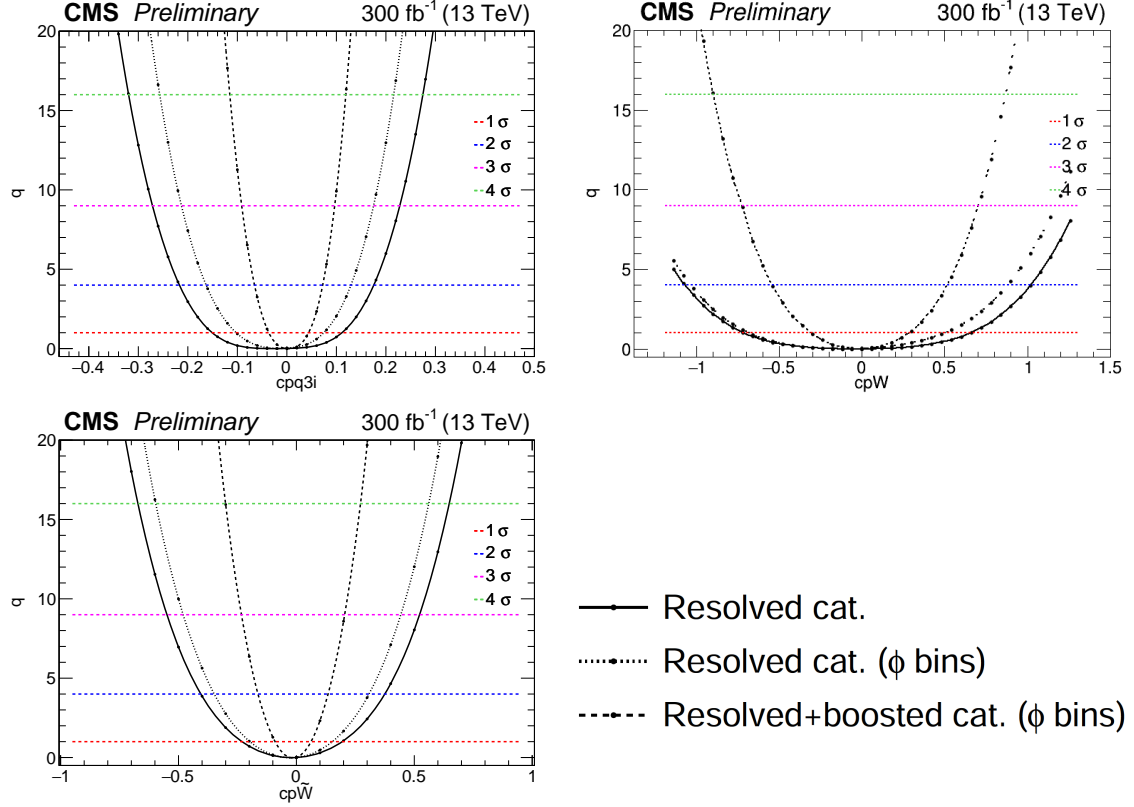


Figure 9: Variation of the profile likelihood ratio $q = -2 \log \frac{L(\vec{\alpha}, \vec{\theta})}{L(\hat{\vec{\alpha}}, \hat{\vec{\theta}})}$, where $\vec{\alpha}$ and $\vec{\theta}$ denote parameters of interest (POIs) and nuisance parameters, respectively, as a function of Wilson coefficients (POIs in this case) corresponding to operators $\mathcal{O}_{Hq}^{(3)}$ (left), \mathcal{O}_{HW} (middle), and $\mathcal{O}_{H\tilde{W}}$ (right) for an integrated luminosity of 300 fb^{-1} .

Table 4: Expected bounds at 68% confidence level on Wilson coefficients corresponding to three operators involved in WH production for integrated luminosity of 300 fb^{-1} .

Operator	Analysis category		
	Resolved	Resolved w/ ϕ bins	Resolved+boosted w/ ϕ bins
$\mathcal{O}_{Hq}^{(3)}$	$[-0.16, +0.11]$	$[-0.1, +0.08]$	$[-0.05, +0.04]$
\mathcal{O}_{HW}	$[-0.80, +0.62]$	$[-0.78, +0.46]$	$[-0.38, +0.26]$
$\mathcal{O}_{H\tilde{W}}$	$[-0.24, +0.22]$	$[-0.22, +0.16]$	$[-0.08, +0.06]$

6.6 Possible extensions of ideas

Here, the proposal is to probe SM-EFT operators in VH production, where V decays to leptons. But, the methodology developed also holds for hadronically decaying V; the only bottleneck in the case of $V = W$ in sensitivity is the absence of knowledge on V

charge. Latest developments in DNN-based methods for vector boson tagging can be used to increase the sensitivity.

Technologies developed for the proposed measurement can also be directly applied to searches with $V \rightarrow \ell^+ \ell^- / \ell \nu$ and $H \rightarrow b \bar{b}$ in the final state, particularly in the context of a heavy resonance decaying to V and H .

7 Planned cooperation arrangement

The work will be conducted within the CMS Collaboration. The reconstructed and simulated data, trigger information, object calibration factors provided centrally by the Collaboration will be used. Ideas and updates will be presented at regular intervals in internal meetings. In general, no cooperative arrangement is planned for this proposal.

However, there are synergies with ongoing activities within the CMS data analysis group at HEPHY. The group recently submitted a paper on measurement of $t\bar{t}\gamma$ process and constraining $t-\gamma$ coupling in SM-EFT; this work was supported by FWF grant P31578. There is also ongoing work on constraining SM-EFT operators in tWZ process supported by FWF grant P33771. Thus the proposed measurement will add a complementary direction in terms of the group's activities.

The CMS data analysis group at HEPHY consists of five staff scientists, three post-doctoral researchers, and five Ph.D. students working on supersymmetry, long-lived signatures, search for BSM Higgs boson decaying to a pair of τ leptons, top quark physics, among others. Diverse experience in the group helps to develop new ideas and implement those in the CMS Collaboration.

8 Work and plan

The work will be carried out by a new Ph.D. student along with the applicant. Since the proposed work is on Higgs physics, which is one of the main centers of activities at LHC, the Ph.D. student will get high visibility within the CMS Collaboration.

Tasks in chronological order are described in the following and summarized in Table 5.

1. Signal simulation for Run 2:

The proposed study requires the simulation of VH events, including the effects of SM-EFT operators both at the levels of production and decay using recently developed software packages, e.g., SMEFTsim [63] at leading-order or using SMEFT@NLO [64] at next-to-leading order in perturbative QCD. Particular care needs to be taken for the matching of generation of the hard process using MADGRAPH5_aMC@NLO [55] and the parton shower with PYTHIA8 [65] since the parton shower does not involve higher-dimensional operators.

2. SM-EFT parameterization:

Information about SMEFT operators will be simulated using a second-order polynomial in the Wilson coefficients involved. A number of weights will be stored for each

event. It needs to be checked if a second-order polynomial is sufficient to parameterize the effects of SM-EFT operators.

3. Optimization of lepton selection:

The conditions used for lepton identification needs to be optimized in such a way that the variation of acceptance for different operators and the total systematic uncertainty are minimized while not compromising on the statistical power of data.

4. Optimization of b tagging condition:

The CMS Collaboration provides the correction to be applied to simulation to match the efficiency of DNN-based b in data and simulation in two variants. The first one, the working point-based method, requires to use certain pre-defined thresholds on b tagging score of a jet to qualified a 'b-tagged' and the corresponding correction has smaller uncertainties. In the second approach, the shape-based method, one can put the threshold at any value in b tagging discriminator and the corrections have larger uncertainties. Since the b tagging information is used for signal-to-background discrimination, it needs to be checked which of the two options provides better overall sensitivity.

5. Optimization of H tagging condition and calculation of correction:

The threshold on the DNN-based H tagging condition needs to be optimized since this is required for signal-to-background separation. Correction factors need to be appropriately calculated to match the tagging efficiency in data and simulation.

6. Trigger efficiency measurement:

The efficiency of lepton-based triggers needs to be measured in both data and simulation. Corrections to match the trigger simulation and data will be derived and applied to the simulation. The same needs to be performed for the backup jet triggers.

7. Neutrino reconstruction:

A careful analysis is required to assign the correct η to the neutrino, which also benefits the CP-sensitivity of the measurements in case of WH production. A powerful prescription developed for neutrino reconstruction will also help similar analyses ongoing in CMS.

8. Background estimation:

In the proposed measurement, the backgrounds are primarily planned to be taken from simulation with a thorough validation by comparing those with data in dedicated control regions. Corrections need to be derived wherever needed, and the corresponding systematic uncertainties need to be quantified.

9. Multivariate analysis:

Modeling of the variables used for signal-to-background separation in DNN-based multivariate analysis and their correlations need to be properly checked. The architecture of the DNN and the threshold of the MVA discriminator need to be optimized. The modeling of the MVA discriminator for different background processes will be checked, and data-to-simulation corrections will be derived if needed.

10. SM-EFT to SM separation:

In the feasibility study, the constraints on Wilson coefficients are derived just by separating events in different regions. A more sophisticated study with larger number of variables and taking into account their correlation needs to be used. This will be a test-bed of a method proposed by the group at HEPHY using boosted decision trees [36].

11. Experimental systematic uncertainties:

Systematic uncertainties related to different objects, e.g. leptons, jets and corrections at event-level need to be applied. The systematic uncertainties need to be properly derived for the corrections developed during this particular analysis.

12. Modeling uncertainties:

Modeling uncertainties in simulation from the choice of renormalization and factorization scales, parton distribution function, parton shower need to be derived and applied to all the predictions taken from simulation. The neutrino reconstruction is also expected to be affected by the modeling uncertainties.

13. Quantification of sensitivity:

Results from different years of Run 2 will be combined and the sensitivity of the analysis will be quantified using likelihood scans, taking into account correlation between the operators. The correlation between systematic uncertainty sources in different years needs to be properly defined. It will be carefully checked if some of the systematic uncertainties are unexpectedly constrained.

14. SM-EFT effects in the background:

So far, all the discussions regarding the SM-EFT operators are made for VH production, which is the signal targeted. However, some of the operators in Table 1 also affect some of the background processes. For example, $\mathcal{O}_{Hq}^{(1)}$, $\mathcal{O}_{Hq}^{(3)}$ affect the diboson production, which is related to VH production by Goldstone boson equivalence theorem at high energy. These are also expected to affect V+jets production. A significant amount of effort needs to be dedicated to the simulation of SM-EFT effects for the backgrounds, followed by a joint analysis of signal and background to report the final sensitivity to the corresponding Wilson coefficients.

15. Publication based on Run 2 data:

A first paper will be written reporting the results based on Run 2 data. This involves a series of reviews within the CMS Collaboration and finally by the journal reviewers.

16. Signal simulation for Run 3:

The setup developed for the signal simulation for Run 2 will be used in Run 3. However, options will be kept open to incorporate the developments in the theory community by this period.

17. Trigger efficiency measurement and optimization of object selection for Run 3:

The triggers which were operational during Run 2 are expected to be available for Run 3 also, but the pileup condition is likely to change. So, the trigger efficiency and corresponding corrections need to be also derived for Run 3. For the same reason, object selection criteria need to be reevaluated for Run 3.

18. Choice of H tagger for Run 3:

With the fast progress in heavy particle tagging, more powerful taggers are expected to be available during Run 3 schedule. An evaluation will be performed based on the available taggers, and the best performant one will be used.

19. Background estimation for Run 3:

Improvements are expected in the Monte Carlo simulation of different processes in the next few years. Thus, the background estimation strategy to be developed for Run 2 analysis will need validation for Run 3.

20. Experimental and modeling systematic uncertainties for Run 3:

Systematic uncertainties due to experimental sources will be added. Modeling uncertainties are expected to be very similar to Run 2.

21. Combination of Run 2 and 3 results:

Results from the analyses based on Run 2 and Run 3 data samples will be combined. Final sensitivity on Wilson coefficients will be reported based on the combined data set.

22. Publication of final results:

The final results will be reported in a paper, which will go through the internal review process by the CMS Collaboration and finally be submitted to the journal for publication.

9 Ethical, safety-related or regulatory aspects

The sole aim of the project is to improve the human understanding of nature. The topic itself has no ethical, safety-related, or regulatory aspects that need to be considered.

10 Sex-specific and gender related issues

The sole aim of the project is to improve the human understanding of nature. Thus the topic itself does not have any gender-related aspects. The job advertisement will be formulated gender neutrally. In order to improve the gender balance at HEPHY ($\sim 20\%$), a suitable female candidate will be given preference.

11 Human resources

A Ph.D. student will be recruited solely for this project to be conducted at HEPHY, Vienna. The Ph.D. student will carry out the project under the supervision of the project applicant, PI Dr. S. Chatterjee. According to the plan, the PI will spend 50% of his time for this project. The PI has five years of experience in CMS data analysis in the context of precision jet measurements, searches for new physics, detector calibration, and implementation of algorithms in the CMS software framework. The PI has also worked on high energy physics phenomenology in collaboration with professional theorists and published papers in international journals.

Tasks will be carried out in consultation with the leader of CMS data analysis group of the institute: Dr. Robert Schöffbeck (RA), who is also performing SM-EFT measurements in top quark physics in association with a post-doctoral researcher Dr. Dennis Schwartz (DS). Cross-talk with RA and DS will be extremely useful for this project. Particularly, the simulation of SM-EFT operators (task 1), SM-EFT parameterization (task 2), and SM-EFT to SM separation (task 10) will be performed together with RA and DS. RA is also the former convener of the 'top quark mass and properties' physics analysis group and the 'jet and MET' physics object group of the CMS Collaboration. His feedback on documentation and presentation of the results will be constructive.

Task / Year	2022 ($\int \mathcal{L} dt \sim 30 \text{ fb}^{-1}$)				2023 ($\int \mathcal{L} dt \sim 120 \text{ fb}^{-1}$)				2024 ($\int \mathcal{L} dt \sim 160 \text{ fb}^{-1}$)			
	Jan-Mar	Apr-Jun	Jul-Sep	Oct-Dec	Jan-Mar	Apr-Jun	Jul-Sep	Oct-Dec	Jan-Mar	Apr-Jun	Jul-Dec	
1. Signal simulation for Run 2	✓											
2. SM-EFT parameterization	✓											
3. Optimization of lepton selection		✓										
4. Optimization of b tagging condition		✓										
5. Optimization of H tagging condition		✓										
6. Trigger efficiency measurement			✓									
7. Neutrino reconstruction			✓									
8. Background estimation				✓								
9. Multivariate analysis				✓								
10. SM-EFT to SM separation					✓							
11. Exp. systematic uncertainties					✓							
12. Modeling uncertainties					✓							
13. Quantification of sensitivity						✓						
14. SM-EFT effects in background						✓						
15. Publication based on Run 2 data								✓				
16. Signal simulation for Run 3							✓					
17. Selections for Run 3							✓					
18. Choice of H tagger for Run 3								✓				
19. Background estimation for Run 3								✓				
20. Systematic uncertainties for Run 3									✓			
21. Combination of Run 2 and 3 results										✓		
22. Publication of final results											✓	

Table 5: Tasks shown using symbol ✓ will be covered by the Ph.D. student, ✓ by the project applicant and Ph.D. student, ✓ by the project applicant and Ph.D. student in collaboration with other members in HEPHY CMS data analysis group.

Annex 1 References

- [1] CMS Collaboration, “The CMS experiment at the CERN LHC”, *JINST* **3** (2008) S08004, [doi:10.1088/1748-0221/3/08/S08004](#).
- [2] ATLAS Collaboration, “Observation of a new particle in the search for the Standard Model Higgs boson with the ATLAS detector at the LHC”, *Phys. Lett. B* **716** (2012) 1, [doi:10.1016/j.physletb.2012.08.020](#), [arXiv:1207.7214](#).
- [3] CMS Collaboration, “Observation of a New Boson at a Mass of 125 GeV with the CMS Experiment at the LHC”, *Phys. Lett. B* **716** (2012) 30–61, [doi:10.1016/j.physletb.2012.08.021](#), [arXiv:1207.7235](#).
- [4] CMS Collaboration, “Measurements of properties of the Higgs boson decaying into the four-lepton final state in pp collisions at $\sqrt{s} = 13$ TeV”, *JHEP* **11** (2017) 047, [doi:10.1007/JHEP11\(2017\)047](#), [arXiv:1706.09936](#).
- [5] CMS Collaboration, “A measurement of the Higgs boson mass in the diphoton decay channel”, *Phys. Lett. B* **805** (2020) 135425, [doi:10.1016/j.physletb.2020.135425](#), [arXiv:2002.06398](#).
- [6] CMS Collaboration, “Constraints on anomalous HVV couplings from the production of Higgs bosons decaying to τ lepton pairs”, *Phys. Rev. D* **100** (2019), no. 11, 112002, [doi:10.1103/PhysRevD.100.112002](#), [arXiv:1903.06973](#).
- [7] CMS Collaboration, “Measurements of $t\bar{t}H$ Production and the CP Structure of the Yukawa Interaction between the Higgs Boson and Top Quark in the Diphoton Decay Channel”, *Phys. Rev. Lett.* **125** (2020) 061801, [doi:10.1103/PhysRevLett.125.061801](#), [arXiv:2003.10866](#).
- [8] B. Grinstein and M. B. Wise, “Operator analysis for precision electroweak physics”, *Phys. Lett. B* **265** (1991) 326, [doi:10.1016/0370-2693\(91\)90061-T](#).
- [9] J.-y. Chiu, F. Golf, R. Kelley, and A. V. Manohar, “Electroweak Corrections in High Energy Processes using Effective Field Theory”, *Phys. Rev. D* **77** (2008) 053004, [doi:10.1103/PhysRevD.77.053004](#), [arXiv:0712.0396](#).
- [10] G. Passarino and M. Trott, “The Standard Model Effective Field Theory and Next to Leading Order”, [arXiv:1610.08356](#).
- [11] E. E. Jenkins, A. V. Manohar, and M. Trott, “Renormalization Group Evolution of the Standard Model Dimension Six Operators I: Formalism and lambda Dependence”, *JHEP* **10** (2013) 087, [doi:10.1007/JHEP10\(2013\)087](#), [arXiv:1308.2627](#).
- [12] R. Alonso, E. E. Jenkins, A. V. Manohar, and M. Trott, “Renormalization Group Evolution of the Standard Model Dimension Six Operators III: Gauge Coupling Dependence and Phenomenology”, *JHEP* **04** (2014) 159, [doi:10.1007/JHEP04\(2014\)159](#), [arXiv:1312.2014](#).
- [13] E. E. Jenkins, A. V. Manohar, and M. Trott, “Renormalization Group Evolution of the Standard Model Dimension Six Operators II: Yukawa Dependence”, *JHEP* **01** (2014) 035, [doi:10.1007/JHEP01\(2014\)035](#), [arXiv:1310.4838](#).
- [14] C. Englert and M. Spannowsky, “Effective Theories and Measurements at Colliders”, *Phys. Lett. B* **740** (2015) 8–15, [doi:10.1016/j.physletb.2014.11.035](#), [arXiv:1408.5147](#).

- [15] I. Brivio and M. Trott, “The Standard Model as an Effective Field Theory”, *Phys. Rept.* **793** (2019) 1, [doi:10.1016/j.physrep.2018.11.002](#), [arXiv:1706.08945](#).
- [16] G. Panico, F. Riva, and A. Wulzer, “Diboson interference resurrection”, *Phys. Lett. B* **776** (2018) 473, [doi:10.1016/j.physletb.2017.11.068](#), [arXiv:1708.07823](#).
- [17] CMS Collaboration Collaboration, “ $W^\pm\gamma$ differential cross sections and effective field theory constraints at $\sqrt{s} = 13\text{ TeV}$ ”, CMS Physics Analysis Summary CMS-PAS-SMP-20-005, 2021.
- [18] S. Banerjee et al., “Towards the ultimate differential SMEFT analysis”, *JHEP* **09** (2020) 170, [doi:10.1007/JHEP09\(2020\)170](#), [arXiv:1912.07628](#).
- [19] S. Weinberg, “Baryon- and lepton-nonconserving processes”, *Phys. Rev. Lett.* **43** (Nov, 1979) 1566, [doi:10.1103/PhysRevLett.43.1566](#).
- [20] F. Bonnet, D. Hernandez, T. Ota, and W. Winter, “Neutrino masses from higher than d=5 effective operators”, *JHEP* **10** (2009) 076, [doi:10.1088/1126-6708/2009/10/076](#), [arXiv:0907.3143](#).
- [21] B. Grzadkowski, M. Iskrzynski, M. Misiak, and J. Rosiek, “Dimension-Six Terms in the Standard Model Lagrangian”, *JHEP* **10** (2010) 085, [doi:10.1007/JHEP10\(2010\)085](#), [arXiv:1008.4884](#).
- [22] K. Hagiwara, R. Szalapski, and D. Zeppenfeld, “Anomalous Higgs boson production and decay”, *Phys. Lett. B* **318** (1993) 155–162, [doi:10.1016/0370-2693\(93\)91799-S](#), [arXiv:hep-ph/9308347](#).
- [23] J. Ellis, V. Sanz, and T. You, “Complete Higgs Sector Constraints on Dimension-6 Operators”, *JHEP* **07** (2014) 036, [doi:10.1007/JHEP07\(2014\)036](#), [arXiv:1404.3667](#).
- [24] C. W. Murphy, “Statistical approach to Higgs boson couplings in the standard model effective field theory”, *Phys. Rev. D* **97** (2018), no. 1, 015007, [doi:10.1103/PhysRevD.97.015007](#), [arXiv:1710.02008](#).
- [25] J. Baglio et al., “Validity of standard model EFT studies of VH and VV production at NLO”, *Phys. Rev. D* **101** (2020) 115004, [doi:10.1103/PhysRevD.101.115004](#), [arXiv:2003.07862](#).
- [26] J. Ellis, V. Sanz, and T. You, “The Effective Standard Model after LHC Run I”, *JHEP* **03** (2015) 157, [doi:10.1007/JHEP03\(2015\)157](#), [arXiv:1410.7703](#).
- [27] C. Grojean, M. Montull, and M. Riembau, “Diboson at the LHC vs LEP”, *JHEP* **03** (2019) 020, [doi:10.1007/JHEP03\(2019\)020](#), [arXiv:1810.05149](#).
- [28] R. S. Gupta, A. Pomarol, and F. Riva, “BSM Primary Effects”, *Phys. Rev. D* **91** (2015), no. 3, 035001, [doi:10.1103/PhysRevD.91.035001](#), [arXiv:1405.0181](#).
- [29] A. Manohar and H. Georgi, “Chiral Quarks and the Nonrelativistic Quark Model”, *Nucl. Phys. B* **234** (1984) 189–212, [doi:10.1016/0550-3213\(84\)90231-1](#).
- [30] H. Qu and L. Gouskos, “ParticleNet: Jet Tagging via Particle Clouds”, [arXiv:1902.08570](#).
- [31] CMS Collaboration, “Identification of heavy, energetic, hadronically decaying particles using machine-learning techniques”, *JINST* **15** (2020) P06005, [doi:10.1088/1748-0221/15/06/P06005](#), [arXiv:2004.08262](#).
- [32] A. Falkowski and F. Riva, “Model-independent precision constraints on dimension-6 operators”, *JHEP* **02** (2015) 039, [doi:10.1007/JHEP02\(2015\)039](#), [arXiv:1411.0669](#).

- [33] S. Banerjee, C. Englert, R. S. Gupta, and M. Spannowsky, “Probing Electroweak Precision Physics via boosted Higgs-strahlung at the LHC”, *Phys. Rev. D* **98** (2018), no. 9, 095012, [doi:10.1103/PhysRevD.98.095012](https://doi.org/10.1103/PhysRevD.98.095012), [arXiv:1807.01796](https://arxiv.org/abs/1807.01796).
- [34] J. Elias-Miro, J. R. Espinosa, E. Masso, and A. Pomarol, “Higgs windows to new physics through d=6 operators: constraints and one-loop anomalous dimensions”, *JHEP* **11** (2013) 066, [doi:10.1007/JHEP11\(2013\)066](https://doi.org/10.1007/JHEP11(2013)066), [arXiv:1308.1879](https://arxiv.org/abs/1308.1879).
- [35] N. Berger et al., “Simplified Template Cross Sections - Stage 1.1”, [arXiv:1906.02754](https://arxiv.org/abs/1906.02754).
- [36] S. Chatterjee et al., “Tree boosting for learning EFT parameters”, [arXiv:2107.10859](https://arxiv.org/abs/2107.10859).
- [37] J. Ellis, C. W. Murphy, V. Sanz, and T. You, “Updated Global SMEFT Fit to Higgs, Diboson and Electroweak Data”, *JHEP* **06** (2018) 146, [doi:10.1007/JHEP06\(2018\)146](https://doi.org/10.1007/JHEP06(2018)146), [arXiv:1803.03252](https://arxiv.org/abs/1803.03252).
- [38] J. Ellis et al., “Top, Higgs, Diboson and Electroweak Fit to the Standard Model Effective Field Theory”, *JHEP* **04** (2021) 279, [doi:10.1007/JHEP04\(2021\)279](https://doi.org/10.1007/JHEP04(2021)279), [arXiv:2012.02779](https://arxiv.org/abs/2012.02779).
- [39] J. J. Ethier et al., “Combined SMEFT interpretation of Higgs, diboson, and top quark data from the LHC”, [arXiv:2105.00006](https://arxiv.org/abs/2105.00006).
- [40] CMS Collaboration, “Constraints on anomalous Higgs boson couplings to vector bosons and fermions in its production and decay using the four-lepton final state”, [arXiv:2104.12152](https://arxiv.org/abs/2104.12152).
- [41] CMS Collaboration, “Probing effective field theory operators in the associated production of top quarks with a Z boson in multilepton final states at $\sqrt{s} = 13$ TeV”, [arXiv:2107.13896](https://arxiv.org/abs/2107.13896).
- [42] CMS Collaboration, “Measurement of the electroweak production of $Z\gamma$ and two jets in proton-proton collisions at $\sqrt{s} = 13$ TeV and constraints on anomalous quartic gauge couplings”, [arXiv:2106.11082](https://arxiv.org/abs/2106.11082).
- [43] “LHC Effective Field Theory WG”. <https://lpsc.web.cern.ch/lhc-eft-wg>.
<https://lpsc.web.cern.ch/lhc-eft-wg>.
- [44] “All Things EFT”. <https://sites.google.com/view/all-things-eft>.
[doi:https://sites.google.com/view/all-things-eft](https://sites.google.com/view/all-things-eft),
<https://sites.google.com/view/all-things-eft>.
- [45] A. G. Cohen, A. De Rujula, and S. Glashow, “A matter - antimatter universe?”, *Astrophys. J.* **495** (1998) 539, [doi:10.1086/305328](https://doi.org/10.1086/305328), [arXiv:astro-ph/9707087](https://arxiv.org/abs/astro-ph/9707087).
- [46] P. H. Damgaard, A. Haarr, D. O’Connell, and A. Tranberg, “Effective Field Theory and Electroweak Baryogenesis in the Singlet-Extended Standard Model”, *JHEP* **02** (2016) 107, [doi:10.1007/JHEP02\(2016\)107](https://doi.org/10.1007/JHEP02(2016)107), [arXiv:1512.01963](https://arxiv.org/abs/1512.01963).
- [47] B. Grzadkowski and D. Huang, “Spontaneous CP -Violating Electroweak Baryogenesis and Dark Matter from a Complex Singlet Scalar”, *JHEP* **08** (2018) 135, [doi:10.1007/JHEP08\(2018\)135](https://doi.org/10.1007/JHEP08(2018)135), [arXiv:1807.06987](https://arxiv.org/abs/1807.06987).
- [48] J. de Blas, M. Chala, M. Perez-Victoria, and J. Santiago, “Observable Effects of General New Scalar Particles”, *JHEP* **04** (2015) 078, [doi:10.1007/JHEP04\(2015\)078](https://doi.org/10.1007/JHEP04(2015)078), [arXiv:1412.8480](https://arxiv.org/abs/1412.8480).
- [49] S. Profumo, M. J. Ramsey-Musolf, C. L. Wainwright, and P. Winslow, “Singlet-catalyzed electroweak phase transitions and precision Higgs boson studies”, *Phys. Rev. D* **91** (2015), no. 3, 035018, [doi:10.1103/PhysRevD.91.035018](https://doi.org/10.1103/PhysRevD.91.035018), [arXiv:1407.5342](https://arxiv.org/abs/1407.5342).

- [50] F. del Aguila, J. de Blas, and M. Perez-Victoria, “Electroweak Limits on General New Vector Bosons”, *JHEP* **09** (2010) 033, [doi:10.1007/JHEP09\(2010\)033](https://doi.org/10.1007/JHEP09(2010)033), [arXiv:1005.3998](https://arxiv.org/abs/1005.3998).
- [51] G. Burdman, B. A. Dobrescu, and E. Ponton, “Resonances from two universal extra dimensions”, *Phys. Rev. D* **74** (2006) 075008, [doi:10.1103/PhysRevD.74.075008](https://doi.org/10.1103/PhysRevD.74.075008), [arXiv:hep-ph/0601186](https://arxiv.org/abs/hep-ph/0601186).
- [52] J. C. Pati and A. Salam, “Lepton number as the fourth color”, *Phys. Rev. D* **10** (1974) 275, [doi:10.1103/PhysRevD.10.275](https://doi.org/10.1103/PhysRevD.10.275).
- [53] F. del Aguila, M. Perez-Victoria, and J. Santiago, “Effective description of quark mixing”, *Phys. Lett. B* **492** (2000) 98, [doi:10.1016/S0370-2693\(00\)01071-6](https://doi.org/10.1016/S0370-2693(00)01071-6), [arXiv:hep-ph/0007160](https://arxiv.org/abs/hep-ph/0007160).
- [54] S. Dawson and E. Furlan, “A Higgs Conundrum with Vector Fermions”, *Phys. Rev. D* **86** (2012) 015021, [doi:10.1103/PhysRevD.86.015021](https://doi.org/10.1103/PhysRevD.86.015021), [arXiv:1205.4733](https://arxiv.org/abs/1205.4733).
- [55] J. Alwall et al., “The automated computation of tree-level and next-to-leading order differential cross sections, and their matching to parton shower simulations”, *JHEP* **07** (2014) 079, [doi:10.1007/JHEP07\(2014\)079](https://doi.org/10.1007/JHEP07(2014)079), [arXiv:1405.0301](https://arxiv.org/abs/1405.0301).
- [56] P. Artoisenet and O. Mattelaer, “MadWeight: Automatic event reweighting with matrix elements”, *PoS CHARGED2008* (2008) 025, [doi:10.22323/1.073.0025](https://doi.org/10.22323/1.073.0025).
- [57] I. Brivio, Y. Jiang, and M. Trott, “The SMEFTsim package, theory and tools”, *JHEP* **12** (2017) 070, [doi:10.1007/JHEP12\(2017\)070](https://doi.org/10.1007/JHEP12(2017)070), [arXiv:1709.06492](https://arxiv.org/abs/1709.06492).
- [58] E. Bols et al., “Jet flavour classification using DeepJet”, *JINST* **15** (2020) P12012, [doi:10.1088/1748-0221/15/12/P12012](https://doi.org/10.1088/1748-0221/15/12/P12012), [arXiv:2008.10519](https://arxiv.org/abs/2008.10519).
- [59] A. J. Larkoski, S. Marzani, G. Soyez, and J. Thaler, “Soft Drop”, *JHEP* **05** (2014) 146, [doi:10.1007/JHEP05\(2014\)146](https://doi.org/10.1007/JHEP05(2014)146), [arXiv:1402.2657](https://arxiv.org/abs/1402.2657).
- [60] CMS Collaboration, “Measurement of $t\bar{t}$ normalised multi-differential cross sections in pp collisions at $\sqrt{s} = 13$ TeV, and simultaneous determination of the strong coupling strength, top quark pole mass, and parton distribution functions”, *Eur. Phys. J. C* **80** (2020), no. 7, 658, [doi:10.1140/epjc/s10052-020-7917-7](https://doi.org/10.1140/epjc/s10052-020-7917-7), [arXiv:1904.05237](https://arxiv.org/abs/1904.05237).
- [61] CMS Collaboration, “Study of Hadronic Event-Shape Variables in Multijet Final States in pp Collisions at $\sqrt{s} = 7$ TeV”, *JHEP* **10** (2014) 087, [doi:10.1007/JHEP10\(2014\)087](https://doi.org/10.1007/JHEP10(2014)087), [arXiv:1407.2856](https://arxiv.org/abs/1407.2856).
- [62] T. Fawcett, “An introduction to roc analysis”, *Pattern Recognition Letters* **27** (2006), no. 8, 861–874, [doi:https://doi.org/10.1016/j.patrec.2005.10.010](https://doi.org/10.1016/j.patrec.2005.10.010). ROC Analysis in Pattern Recognition.
- [63] I. Brivio, “SMEFTsim 3.0 — a practical guide”, *JHEP* **04** (2021) 073, [doi:10.1007/JHEP04\(2021\)073](https://doi.org/10.1007/JHEP04(2021)073), [arXiv:2012.11343](https://arxiv.org/abs/2012.11343).
- [64] C. Degrande et al., “Automated one-loop computations in the standard model effective field theory”, *Phys. Rev. D* **103** (2021) 096024, [doi:10.1103/PhysRevD.103.096024](https://doi.org/10.1103/PhysRevD.103.096024), [arXiv:2008.11743](https://arxiv.org/abs/2008.11743).
- [65] T. Sjstrand et al., “An Introduction to PYTHIA 8.2”, *Comput. Phys. Commun.* **191** (2015) 159, [doi:10.1016/j.cpc.2015.01.024](https://doi.org/10.1016/j.cpc.2015.01.024), [arXiv:1410.3012](https://arxiv.org/abs/1410.3012).

Annex 2 Research institution and required funding

The Institute of High Energy Physics (HEPHY) of the Austrian Academy of Sciences was founded in 1966. Its main purpose is the research in high energy physics and to exploit Austria's membership at CERN. On the hardware side, HEPHY has made significant contributions to the CMS inner tracker and to the trigger system. The CMS data analysis group, led by Dr. R. Schöffbeck, consists of 14 members based at offices in the Apostelgasse 23 in Vienna and at CERN. The successful candidate will be based in Vienna. This choice will enable a direct collaboration with the other Ph.D. students and two master students doing data analysis in CMS, as well as with the scientist of the New Physics theory group. Additionally, four members are based at CERN. Among them is Dr. W. Adam, the former physics coordinator of the CMS experiment and the leader of HEPHY team at CERN.

The infrastructure available to the HEPHY CMS analysis group comprises:

- Office space with personal workstations at Apostelgasse 23.
- Access to an LHC-Grid (LCG) Tier-2 cluster with 1000 CPU cores and 500 TByte storage. Access to the CLIP computing cluster at the Gregor Mendel Institute of the Austrian Academy of sciences with approx. 10k CPU cores and 50 TB of storage for analysis work.
- Video-conferencing equipment for daily communication with other CMS physicists and for participation in meetings in the CMS collaboration.

This project application requests funding for one Ph.D. student for 36 months (EUR 39.780 per year in 2021). The PI S. Chatterjee is a post-doctoral researcher at HEPHY. Upon a positive funding decision by the FWF, a call for the Ph.D. student will be opened, advertised inside and outside Austria, and made equally accessible to physicists regardless of their race, color, creed, national origin, religion, family status, sexual orientation, age, and political beliefs. In order to improve the gender balance at HEPHY ($\sim 20\%$), a suitable female candidate will be given preference.

Furthermore, a total of EUR 5.155 per year for travel expenses between Vienna and CERN is requested. These costs are justified as follows: The Ph.D. student will travel four times a year (approximately every two months) to CERN for, on average, one week. The purpose of four trips is the collaboration with the other experimentalists in the CMS HIG group and to present in person to the other members of the CMS collaboration. Also, the Ph.D. student will get an opportunity to participate in the detector operation during the data-taking periods. If possible, the CERN trips will overlap with a CMS collaboration week (internal CMS working meeting occurring four times a year at CERN). Furthermore, one trip to the annual Higgs conference is foreseen, where recent developments in experimental and theoretical results on the Higgs boson are presented. Cost for this trip is assumed to be the same as for a trip to CERN. A breakdown of the expected costs of a working travel to CERN is provided in Table 6.

The institute needs to pay an amount (MoE) for the PI, which amounts to EUR 10.000 per year, this is also requested in the proposal. An extra 5% of the total that amounts to

Table 6: Estimation of travel costs for trips to CERN.

Item	Cost	Comment
Flight VIE-GVA-VIE	EUR 300	
7 per diem at EUR 28,10	EUR 196,70	
7 per noctem at EUR 24,90	EUR 174,30	
6 hotel nights at EUR 60	EUR 360	
Total per year	EUR 5.155	5 trips per year
Total	EUR 15.465	For 3 years in total

Table 7: Total amount of requested funding.

Item	Cost
Ph.D. student's salary	EUR 119340
Ph.D. student's travel costs of	EUR 15465
MoE of the PI (for 3 years)	EUR 30000
General costs (5%)	EUR 8240
Total	EUR 173045

EUR 164805 is requested to cover other unexpected costs. Total requested funding sums up to EUR 173045. A summary of the total costs of the project is provided in [Table 7](#).

Annex 3 CV of the principal investigator

Personal Data

Age: 27 years (as of February 1, 2021)

Nationality: Indian

Sex: Male

Affiliation: Institute of High Energy Physics of the Austrian Academy of Sciences, 1050 Vienna

Designation: Post-doctoral researcher

Contact Details

Email: suman.chatterjee@oeaw.ac.at, suman.chatterjee@cern.ch

Phone: +91-7710835260, +43-6769390476

Personal website: <https://sumanchatterjeetifr.wordpress.com>

Academic Records

2016-2020: Ph.D. in Experimental Particle Physics

Department of High Energy Physics

Tata Institute of Fundamental Research, Mumbai 400005, India

Ph.D. Supervisor: Prof. Gobinda Majumder

2014-2016: Master of Science in Physics (Rank: 1st)

Tata Institute of Fundamental Research, Mumbai 400005, India

2011-2014: Bachelor of Science in Physics (Remark: 1st class)

Department of Physics

Jadavpur University, Kolkata 700032, India

Achievements

- | | |
|-------------|---|
| 2020 | Honorable mention for the IPA Rahul Basu Memorial Award for Best Thesis in High Energy Physics for the period 2018–2020 in XXIV DAE-BRNS HEP Symposium 2020, India |
| 2015 | Professor Sukumar Biswas Ph.D. Student Award for Excellence in Physics for scoring the highest grades in graduate courses in the Physics Integrated Ph.D. program in Tata Institute of Fundamental Research |
| 2014 | All India Rank 3 in Joint Entrance Screening Test 2014 conducted by the research institutes in India |
| 2011 | Awarded by the Chief Minister of the state of West Bengal for securing the 4th rank in the state in Higher Secondary (10+2) Examination (conducted by West Bengal Council for Higher Secondary Education) |

Oral Presentations at Conferences, Workshops

September 2021 Joint annual meeting of Austrian and Swiss physical societies, Innsbruck, Austria

Parallel talk SM-EFT results in Higgs sector from the CMS experiment

July 2021 European Conference on High Energy Physics 2021, Hamburg, Germany (online)

Parallel talk Jet substructure measurements in CMS

Dec 2020 XXIV DAE-BRNS HIGH ENERGY PHYSICS SYMPOSIUM 2020

Rahul Basu Memorial Thesis Award Seminar Jets as probes for precision measurement and candles for physics beyond standard model

Jan 2020 QCD with Electron-Ion Collider, IIT Bombay, Mumbai, India

Plenary talk Understanding parton distribution function from LHC measurements

Sep 2019 Workshop on Top Quark Physics 2019, IHEP, Beijing, China

Invited talk Heavy resonance searches in ATLAS and CMS

July 2019 European Conference on High Energy Physics 2019, Ghent, Belgium

Parallel talk Inclusive jet results from CMS experiment

July 2019 European Conference on High Energy Physics 2019, Ghent, Belgium

Parallel talk Tagging top in leptonic decay

Feb 2019 International Workshop on Forward and Jet Physics at LHC, Bose Institute, Kolkata, India

Invited talk Measurement of inclusive jet cross section and event properties in CMS experiment

Aug 2018 QCD at LHC 2018, Technische Universität Dresden, Dresden, Germany

Parallel talk LHC top quark and jet measurements sensitive to PDFs

Aug 2018 QCD at LHC 2018, Technische Universität Dresden, Dresden, Germany

Parallel talk Differential jet cross sections at the CMS experiment

Dec 2017 Workshop on High Energy Physics Phenomenology XV, IISER Bhopal, Bhopal, India

Parallel talk Radius Scan for Inclusive Jets in CMS Experiment at $\sqrt{s} = 13$ TeV

Dec 2016 XXII DAE-BRNS High Energy Physics Symposium, Delhi, India

Parallel talk Perspectives for a Radius Scan in Inclusive Jets at 13 TeV with CMS

Poster Presentations

June 2021 Large Hadron Collider Physics (LHCP 2021) conference, Paris, France (online)

Search for W' bosons decaying to a top and a bottom quark at $\sqrt{s} = 13$ TeV

Sep 2018 Asia-Europe-Pacific School on High Energy Physics, Quy Nhon, Vietnam

Radius scan for inclusive jets at $\sqrt{s} = 13$ TeV

Teaching Experience

Autumn 2019: Teaching assistant

Course: Statistical Methods in Physics at TIFR, Mumbai

January 2019: Co-coordinator

Lecture and hands-on exercise on algorithms used in particle physics for event generation, object reconstruction, and analysis at the XII School on Experimental High Energy Physics conducted by the Science and Engineering Research Board in India at TIFR, Mumbai

Autumn 2016: Teaching assistant

Course: Advanced Electrodynamics at TIFR, Mumbai

Supervision Experience

Anirban Bala (Ph.D. student at TIFR, Mumbai, Advisor: Prof. M. Guchait):

During his departmental project I (July-September, 2020) under Prof. G. Majumder

Designed the project and mentored thoroughly during its implementation

Organizational Responsibilities

XII School on Experimental High Energy Physics at TIFR, Mumbai

Helped the organization at the institute level

SUSY 2017 conference at TIFR, Mumbai

Led the team of volunteers

Selected Publications

1: *Search for a W' boson decaying to a top and a bottom quark at $\sqrt{s} = 13$ TeV*

CMS Collaboration

Phys. Lett. B 820 (2021) 136535

Most stringent limits published to date on right- and left-handed W' bosons decaying to a top and a bottom quark.

2: *Dependence of inclusive jet production on the anti- k_T distance parameter in pp collisions at $\sqrt{s} = 13$ TeV*

CMS Collaboration

JHEP 12 (2020) 082

First public results from colliders on dependence of inclusive jet cross section on jet size.

3: *Calibration of the CMS hadron calorimeters using proton-proton collision data at $\sqrt{s} = 13$ TeV*

CMS Collaboration

JINST 15 (2020) P05002

Absolute calibration of outer hadron calorimeter in particle-flow algorithm in CMS.

4: *Jets with electrons from boosted top quarks*

Suman Chatterjee, Rohini Godbole, and Tuhin S. Roy

JHEP 01 (2020) 170

An algorithm to identify boosted top quarks decaying where W boson from top quark decays to an electron using jet substructure techniques.

5: *Mixed WIMP-axion dark matter*

Suman Chatterjee, Anirban Das, Tousik Samui, and Manibrata Sen

Phys. Rev. D 100, 115050

A detailed study of the phenomenology of a multi-component dark matter scenario with a scalar WIMP and the QCD axion in the light of the latest data from dark matter detection experiments and LHC results.

6: *Dose rate effects in the radiation damage of the plastic scintillators of the CMS hadron endcap calorimeter*

CMS Collaboration

2016 JINST 11 T10004

Measurements of change in light output by plastic scintillators in the CMS hadron endcap due to irradiation during the collisions at LHC at $\sqrt{s} = 8$ TeV.